

High-Pressure Stability in Ordered Mesoporous Silicas: Rigidity and Elasticity through Nanometer Scale Arches

Junjun Wu, Xiaoyang Liu, and Sarah H. Tolbert*

Department of Chemistry and Biochemistry, University of California, Los Angeles,
Los Angeles, California 90095-1569

Received: August 15, 2000; In Final Form: October 25, 2000

High-pressure, low-angle X-ray diffraction is used to examine the compressibility of periodic hexagonal, surfactant-templated silicas. Mesoscopic order in these materials can be retained up to 12 GPa, and pressure-induced distortions are reversible. Postsynthetic treatments can greatly enhance the mechanical properties of these nanostructured materials. Bulk moduli equal to and even higher than values measured for bulk vitreous silica are obtained if both the nanometer-scale order and local atomic-scale bonding are optimized. The results show that common architectural motifs, such as the arch or the honeycomb structure, can be used to produce rigidity and elasticity without excessive mass in materials with periodicity down to mere nanometers.

The search for materials that are light but mechanically robust has historically focused on organic-based materials such as polymers or carbon fiber composites. While remarkable strength and elasticity can be generated in these materials, stability at extreme temperature conditions is limited by the chemical nature of the organic matrix. Porous inorganic materials such as disordered sol–gel glasses, by contrast, are light and can have good high- and low-temperature stability, but under an applied force these materials are both compressible and irreversibly deformed. For example, while disordered sol–gel glasses can be annealed to locally cross-link the silica, these materials are always fairly weak, probably due to their overall fractal geometry.^{1,2} Disordered sol–gel glasses have been studied for a variety of applications that exploit their high porosity, including low mass, low thermal conductivity, and low dielectric constant.³ The fragility of these porous materials, however, limits their effectiveness for many of these applications.

In this paper, we show that many of these problems can be alleviated using periodic surfactant templated silicas. By moving from a disordered porous glass to a nanoscale honeycomb structured material, we find that a significant increase in both bulk modulus and volume elasticity at high pressure can be achieved—in some cases surpassing the rigidity and elasticity of the bulk material. The results indicate that structural properties may be directly controlled by nanoscale architecture and that chemical control over both atomic and nanometerscale structure can be used to optimize material properties.

In the experiments ordered silica/surfactant composites⁴ or calcined mesoporous silicas⁴ were compressed using conventional diamond anvil cell techniques.⁵ An inert, dry pressure medium (liquid/solid Ar) was used to ensure hydrostatic conditions. The shift in the low-angle diffraction peak position with pressure was used to calculate the volume compressibility (or its inverse, the bulk modulus [κ]). The results of measurements made on *P6mm* periodic surfactant-templated silicas suggest that ideal nanometer scale architecture can result in mesostructured silicas with both rigidity and elasticity under high pressure.

Periodic silica/surfactant composites were synthesized by established wet chemical techniques.^{4,6,7} Alkyltrimethylammonium bromide surfactants of two different alkyl chain lengths (16- and 20-carbons) were used to synthesize the silica/surfactant composites under basic conditions. Composites made with 20-carbon chain surfactants were used as synthesized.⁷ Composites made with 16-carbon chain surfactants were either used as synthesized or were hydrothermally treated to improve nanometer-scale order and framework condensation.⁶ In a typical reaction 0.310 g of surfactant was dissolved in 10.0 g of water with the addition of 0.926 g of 2.00 mol/kg NaOH solution. Then 0.788 g of tetraethyl orthosilicate (TEOS) was added, and the mixture was stirred for 30 min. The product was filtered, washed, and air-dried. During hydrothermal treatment, samples were slurried with water and heated at 100 °C for 4 days in a sealed vessel. Mesoporous silicas were generated from the hydrothermally treated materials by calcination, which typically involved first ramping the temperature from 25 to 500 °C at 1 °C/min under N₂, holding the temperature at 500 °C under flowing N₂ for 6 h, and finally holding under flowing O₂ at 500 °C for an additional 6 h. Sample density was determined using an Accupyc 1330 from Micromeritics. The overall density of hydrothermally treated silica/surfactant composites was found to be 1.26 ± 0.01 g/cm³. The density of calcined mesoporous silicas (silica framework only) was measured at 2.02 ± 0.03 g/cm³, a value that is close to the density of bulk vitreous silica (2.2 g/cm³).

High-pressure compressibility and stability were measured using small-angle X-ray diffraction (XRD) to follow the position and intensity of the low-angle diffraction peaks that result from the ordered nature of the surfactant domains or pores. Diffraction patterns were collected using a Roper Scientific X-ray CCD camera. Either an in-house rotating anode X-ray generator (Mo K α radiation, 17.4 keV) or beamline 10-2 at the Stanford Synchrotron Radiation Laboratory (13.0 keV) was used for the X-ray source. ²⁹Si magic angle spinning nuclear magnetic resonance spectroscopy (MAS NMR) was used to probe the degree of inorganic condensation and the degree of disorder in the silica frameworks. Experiments utilized a Bruker MSL 300 spectrometer (7.05 T field) with a standard one pulse acquisition

* To whom correspondence should be addressed: tolbert@chem.ucla.edu.

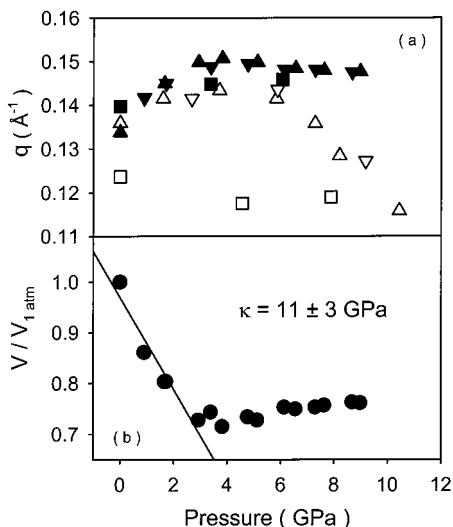


Figure 1. (a) Dependence of the (100) diffraction peak position (q_{100}) on pressure for ordered silica/surfactant composites synthesized with a 20-carbon chain trimethylammonium surfactant. Empty symbols indicate samples dried in air. Filled symbols show the behavior of materials dried under vacuum. In all cases, triangles indicate data collected with increasing pressure while squares indicate data collected upon release of pressure. The shift to lower q at high pressure in the air-dried samples is indicative of structural collapse related to residual water left in this material. (b) The solid data from part a (vacuum-dried composite) can be used to calculate a fractional volume change with pressure. A linear fit to the low-pressure data is used to measure the volume compressibility or bulk modulus of the composite.

using a $5.2 \mu\text{s}$ $\pi/2$ pulse, an $8.8 \mu\text{s}$ dead-time delay, and a 240 s recycle delay. By correlating the results of ^{29}Si MAS NMR with high-pressure XRD, we were able to gain an understanding of the relationship between local bonding and nanometer scale order in determining the material's stiffness.

When silica/surfactant composites are subjected to elevated pressures, the low-angle diffraction peaks are observed to shift to higher q , corresponding to a decreasing nanometer scale repeat distance. Figure 1a (open symbols) shows data for an as-synthesized material made with a 20-carbon chain trimethylammonium surfactant. The peak position increases up to about 4 GPa but then turns over and starts to shift toward lower angle with increasing pressure (Δ , ∇). This decrease is not indicative of a pressure-induced expansion but rather of collapse of the nanometer scale periodicity under pressure.⁸ Upon release of pressure (\square) the peak position does not return to its original value, indicating that pressure-induced collapse is not reversible.

The poor high-pressure stability of these composites can be correlated with residual water left in the material after air-drying at room temperature. Water has been shown to be a requirement for initiation of phase transitions or other structural rearrangements in silica/surfactant composites.^{7,9} Water also accelerates phase transitions in bulk silicates under high pressure.¹⁰ Similarly, calcined mesoporous silicas that are not protected from water have been shown to collapse at low pressure when compressed with a uniaxial load.¹¹ The mechanical strength under uniaxial load improves, however, when the silica surface is protected from water with a monolayer of silane molecules.¹²

When excess water is removed by drying the composites at room temperature under a vacuum of about 0.4 mTorr for 12 h, more predictable behavior occurs under pressure. A fairly linear shift to higher angle is observed up to 4 GPa, followed by a flattening which continues up to 9 GPa (Figure 1a, solid symbols). Similar data are observed up to 12 GPa. When pressure is released, the q_{100} position of the vacuum-dried sample

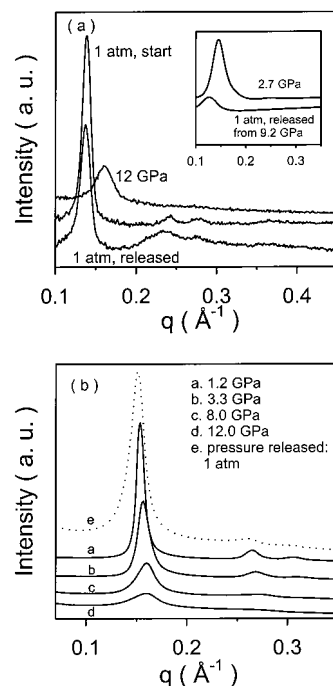


Figure 2. (a) High-pressure X-ray diffraction patterns for ordered, vacuum-dried silica/surfactant composites synthesized with a 20-carbon chain trimethylammonium surfactant. While the quality of the diffraction pattern decreases at high pressure, it recovers upon release of pressure. Inset: high-pressure X-ray diffraction patterns for the same sample dried only in air. Because of water-induced chemistry, this material does not recover its intensity upon release of pressure. (b) High-pressure X-ray diffraction patterns for a silica/surfactant composite synthesized with a 16-carbon chain trimethylammonium surfactant and hydrothermally treated to increase silica condensation. Again, a loss of diffraction intensity is observed at high pressure, which recovers upon release of pressure.

is reversible, retracing the changes in peak position observed with increasing pressure. This reversibility indicates that pressure-induced collapse (Figure 1a, open symbols) can be associated solely with the effect of water and is not intrinsic to the silica framework of these materials.

We assign the lack of a shift in diffraction peak position with pressure above 4 GPa to distortion of the silica framework. Evidence for this distortion can be seen in Figure 2a. When a dry composite is compressed to 12 GPa, the intensity of the diffraction peak decreases significantly, the peak width broadens, and the higher order diffraction peaks disappear. When the pressure is fully released to 1 atm, however, the mesoscopic ordering of the composite is well recovered ($\sim 75\%$ recovered). For samples that were not dried under vacuum, the peak intensity stays low, near its highest-pressure value upon release of pressure (Figure 2a, inset), indicating that for damp samples, nanoscale distortions are coupled to irreversible chemical changes in the silica framework.

While elastic deformation of dry surfactant templated silica makes reasonable chemical sense, it is not in full agreement with data that have been collected on bulk silica glass. It is known that below about 8 GPa changes in the volume of solid vitreous silica with pressure are reversible.¹³ Elastic compression within this pressure range occurs through bending of the Si—O—Si intertetrahedral angles.¹³ Above 8 GPa, however, bulk silica densification becomes irreversible.¹⁴ These irreversible changes are again assigned to bond angle distortions, but at these higher pressures metastable configurations of the bulk silica are accessed, which cannot revert to the original state upon release of pressure.¹⁵ Although pressures as high as 12 GPa are reached

with vacuum-dried composites, the data for these samples still show good reversibility upon release of pressure, a result not observed for bulk material.

To compare our data more effectively with data obtained on bulk silica, the linear compressibility presented in Figure 1a can be converted to volume compressibility. To do this, however, we must make assumptions about the linear compressibility in the hexagonal *c*-direction (along the channels), which is not measured in the experiment. While the unique axis is usually considered to be the strong direction of a hexagonal honeycomb structure,¹⁶ we assume that the compressibility in this unique direction is the same as that in the hexagonal plane. That is, we assume that $V/V_0 \propto (d/d_0)^3$ where V_0 and d_0 are the atmospheric pressure unit cell volume and *d*-spacing, respectively. The result of this assumption is that the numbers we calculate are an upper limit on the compressibility and indicate a softer structure than the one that actually exists.

Figure 1b shows the change in unit cell volume with pressure for a vacuum-dried composite. In the low-pressure regime (up to about 3 GPa), the data show a fairly linear volume decrease. Above this pressure, the composite hardens and the shift to smaller volume with increased pressure ceases. This type of data is also observed in bulk silica glass where the compressibility is found to be fairly constant (although slightly increasing) up to about 4 GPa, after which point the glass becomes much stiffer.¹⁷ The volume compressibility can be obtained from a linear fit to the low-pressure region. The data are reported here as the inverse compressibility or the bulk modulus. While fits to molecularly based equations of state are more commonly used to calculate both κ and its derivative with respect to pressure, the quality of the data and the supermolecular origin of our diffraction peaks do not justify such analysis. A value of $\kappa = 11 \pm 3$ GPa is obtained for our composites. This number should be compared to the average value of the bulk modulus in the pressure range 0–3 GPa for solid fused quartz ($\kappa = 32$ GPa)¹⁸ and crystalline α -quartz ($\kappa = 46$ GPa).¹⁹ By contrast, a bulk modulus of 2.8 GPa is measured for disordered silica aerogels with approximately the same inorganic fraction as the materials used here.¹ The results show that the rigidity of the ordered composite, while 3x lower than solid silica glass, is still much higher than the disordered porous material. If a 16-carbon tail trimethylammonium surfactant is used instead of the 20-carbon tail in the synthesis of the composite, the bulk modulus of the resulting material is 16 ± 3 GPa. Materials with smaller organic domains appear to be somewhat stiffer, but the effect is not extremely large.

To understand our measured mesophase κ values, we need to consider the intrinsic compressibilities of both the silica and the surfactant components of the composite. The compressibility of micellar aggregates in aqueous solutions can be measured by sound–velocity measurements.²⁰ For a micellar solution of a 12-carbon trimethylammonium surfactant, the modulus is 2.4 GPa. The surfactants used in our experiments are expected to have similar moduli values. This low modulus for the micellar aggregates indicates that the silica framework dominates the compressive strength of these materials. Optimizing the strength of the frame should thus result in a stronger material.

Hydrothermal treatment of silica/surfactant composites has been used to improve ordering and polymerization of the silica framework, as shown by low-angle XRD and MAS ²⁹Si NMR.⁶ Figure 3a shows the shift in diffraction peak position with pressure for a composite made with a 16-carbon tailed surfactant and then annealed in water at 100 °C, followed by vacuum-drying. The peak position is observed to shift smoothly to higher

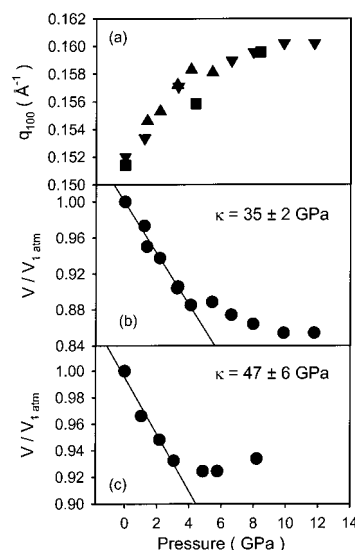


Figure 3. (a) Dependence of the (100) diffraction peak position (q_{100}) on compressive pressure for vacuum-dried, ordered silica/surfactant composites synthesized with a 16-carbon chain trimethylammonium surfactant and hydrothermally treated for 4 days at 100 °C. Triangles indicate data collected with increasing pressure, while squares indicate data collected upon release of pressure. Good reversibility of peak position is found upon release of pressure. (b) The data from part a can be used to calculate a fractional volume change with pressure for the composite. (c) Fractional volume change with pressure for a mesoporous silica produced by calcination of the composite used for parts a and b. A linear fit to the low-pressure data in both parts b and c is used to measure the volume compressibility or bulk modulus of the composite.

q (lower *d* spacing) with increasing pressure (triangles). No roll-over in peak position, indicative of structural collapse, is observed, although the slope of the *q* versus *P* curve does decrease at the highest pressures. When the pressure is released (squares), the peak position exactly tracks the increasing pressure data.

Examination of the raw data (Figure 2b), however, indicates that again the quality of the diffraction pattern decreases at elevated pressures but recovers when pressure is released. While the higher-order diffraction peaks are slightly less intense in the recovered pattern, the higher-order peaks can still be clearly observed, and the fundamental diffraction peak recovers both peak position and most of its intensity. The result emphasizes the fact that silica/surfactant composites do not undergo significant irreversible pressure-induced changes up to 12 GPa despite the fact that irreversible changes are observed in bulk silica at these pressures. An explanation for this fact may lie in the nanoscale nature of these materials. As discussed above, the irreversible densification in bulk silica has been assigned to the formation of metastable structures under pressure that cannot revert upon release of pressure.¹⁵ The finite extent of the silica domains may lower activation energies for reversion and thus allows the nanometer-scale material to spring back to its original form while the bulk material is kinetically trapped in the dense, compressed structure.²¹

Evidence that densification processes similar to those occurring in bulk materials are also occurring in our nanoscale materials can be found by further examination of Figures 1 and 3. The gradual densification of bulk silica under pressure (both reversible and irreversible) has been assigned to a low-density-amorphous (LDA) to high-density-amorphous (HDA) phase transition.²¹ In the bulk, it is postulated that this transition occurs in different sized domains at different pressures, resulting in a gradual stiffening of the solid above 4 GPa.^{15,21} The sharp

decrease in compressibility in all materials at 4 GPa (Figures 1 and 3) may be a result of this atomic scale phase transformation that is occurring nearer to its thermodynamic transition point in these nanoscale materials. The distortion of the nanometer scale periodicity at high pressure (and its recovery) could then result from this reversible atomic scale phase transition.

When the linear compressibility of the hydrothermally treated sample in the low-pressure regime is converted to volume compressibility, the results are quite surprising. The measured bulk modulus of $\kappa = 35 \pm 2$ GPa is within experimental error of the value obtained for solid vitreous silica.¹⁸ The discovery of bulklike rigidity in a material that is less than 40% inorganic and which has a density of only 1.26 g/cm³ is a remarkable contrast to disordered porous inorganics, which are also light, but easily compressed.¹ This result also indicates that common architectural motifs—such as the arch or the honeycomb, which are used to produce rigidity without excessive mass in bulk materials²²—are valid concepts down to the nanometer length scale.

While the results for hydrothermally treated silica/surfactant composites are quite promising, the lightest materials that can be made are calcined, porous silicas. Because calcination is a high-temperature process, it serves not only to remove the organic template but also to increase condensation of the silica framework.²³ The XRD patterns of calcined samples as a function of pressure follow trends similar to those seen in hydrothermally treated samples with fairly linear compressibility observed up to 4 GPa. Upon release of pressure from 8 GPa the peak position returns to its atmospheric pressure value.

Although the surfactant has been removed from these samples, the high-pressure experiment is actually quite similar to those on the surfactant containing materials because here, too, the pores are not empty. On the basis of changes in diffraction peak intensities, we can conclude that the Ar pressure medium fills the pores during cryogenic loading (when the Ar is liquid). After solidification, the Ar acts much like the surfactant: it is a soft solid with a high compressibility.²⁴ As the bulk modulus of solid Ar is fairly low ($\kappa_0 = 6.5$ GPa²⁴), the main difference between the Ar and the surfactant as a pore-filling medium is that the surfactant favors the hexagonal arrangement of the pores based on electrostatic considerations. The Ar, by contrast, does not favor any specific nanometer scale architecture and lacks strong electrostatic interaction between the pore-filling molecules and the pore surface. Experiments to assess the specific role of Ar and other pore-filling materials in stabilizing mesoporous silicas under pressure are currently underway. High-pressure diffraction experiments performed on zeolites with pressure media that were slow to diffuse into the very small pores, however, confirm the notion that the degree of pore filling can significantly affect the high-pressure stability of porous materials.²⁵

Given the nondirectional nature of the Ar–silica interactions, it is somewhat surprising that the bulk modulus of the calcined porous sample is greater than the bulk modulus of the hydrothermally treated composite. A linear fit to the low-pressure region in Figure 3c generates a bulk modulus of 47 ± 6 GPa, a value close to the number obtained for bulk crystalline quartz and higher than the value obtained for bulk silica glass. While this high value may be due in part to the slightly higher bulk modulus of solid Ar compared to the surfactant,^{20,24} the result may also be a manifestation of the unique stabilization that can be found in finite materials. Simulations²⁶ and experiments²⁷ on nanoscale wires have found that finite materials can be much stronger than the bulk material. The result is ascribed to a

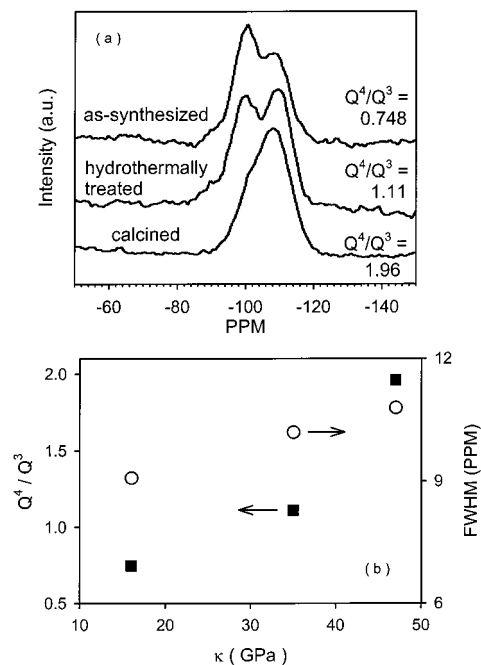


Figure 4. (a) ²⁹Si MAS NMR spectra of ordered silica/surfactant composites after different treatments. In all cases, a 16-carbon chain trimethylammonium surfactant was used as the template. Sample treatments are indicated on the figure. (b) Relation between the Q^4/Q^3 ratio, the full width at half-maximum of the Q^4 peak, and the bulk moduli of the composites after different treatments. More condensed materials are observed to have a higher bulk moduli. The increase is not due to increased ordering because these materials also have broader NMR peaks.

reduction in defect density in these finite systems. Materials fail at the weakest point, which is almost always a defect or grain boundary. Because it is kinetically feasible for defects to migrate to the surface in finite systems, nanostructured materials can be more perfect on the interior and thus stronger than the bulk material.^{26,27} The observation of a compressive modulus approximately equal to that of crystalline silica in a material with an amorphous silica framework may be one manifestation of the mechanical enhancements found in nanoscale materials. While we realize that the concept of defect density is not well-defined in an amorphous material such as the composites under study here, the idea may be interpreted simply in terms of degree of cross-linking or bond strain.

To examine changes in local bonding in these composite and porous materials, we turn to ²⁹Si MAS NMR. Figure 4a presents NMR spectra for materials similar to those used in Figure 1, Figure 3a,b, and Figure 3c. In all cases only two peaks are present. The peak near -110 ppm is assigned to fully condensed silica [Q^4 silica, $\text{Si}-(\text{O}-\text{Si})_4$]. The peak at -100 ppm corresponds to either a defect or an interface [Q^3 silica, $\text{HO}-\text{Si}-(\text{O}-\text{Si})_3$]. The amount of Q^3 silica is always quite high because of the large surface area in these materials. As the degree of polymerization increases, however, the bulk modulus of the composite also increases. Figure 4b (solid symbols), shows a roughly linear relationship between the measured Q^4/Q^3 ratio and bulk modulus. This result suggests that the rigidity of these materials can be directly related to the degree of condensation of the framework.

A second possible type of stabilization that has been postulated for amorphous materials is that of intermediate range order.²⁸ The disordered nature of silica glass is not the result of variation in Si–O bond distance but rather variation in the inter-tetrahedral Si–O–Si bond angle distribution. If this

Si—O—Si bond angle distribution was reduced, the result would be a more ordered solid with less strained bonds. It is known that the ^{29}Si MAS NMR spectrum can be transformed into the Si—O—Si bond angle distribution²⁹ with the width of the NMR peak being proportional to the width of this distribution. As shown in Figure 4b (open symbols), the width of the NMR peaks actually broaden on going from the least condensed to the most condensed materials. It is thus evident from these results that medium range order does not account for the observed increase in rigidity of the composites after hydrothermal treatment. The more important factor is simply the degree of polymerization in the silica framework.

The concept of a nanometer-scale arch dramatizes the idea that atomic and molecular building blocks can be used to construct complex, rigid structures on the nanoscale in much the same way that bricks are used on the macroscale. On a more practical level, however, the combination of lightweight, low- and high-temperature stability, and oxidative stability indicates that ordered inorganic/organic composites and porous inorganics could provide a viable alternative to disordered sol-gel based materials in places where rigidity or reversible deformation is important. A specific example is the use of these materials in low-dielectric coatings.^{30–32} Particularly in areas like the aerospace industry, where low mass and extreme temperature stability need to be combined, the potential for porous silica based materials is exciting. On the high-temperature end, the nanometer-scale architecture in these materials has been shown to be stable up to 800 °C.³³ Although extreme temperatures do not damage these materials, we have shown that water can dramatically reduce the material's strength. In particular, the calcined porous material is very sensitive to moisture. Silylation with hydrophobic organic groups, however, can be used to restrict access of water to the surface and thus reduce hydrolysis-induced degradation.¹² The simple fact that nanostructured silicas can be both stiffer and more elastic than the fully dense solid opens up a new dimension to the design of lightweight structural materials.

Acknowledgment. The authors wish to thank A. F. Gross for help with sample preparation and solid state NMR. This manuscript contains work performed at the Stanford Synchrotron Radiation Laboratory (SSRL), which is operated by the Department of Energy, Office of Basic Energy Sciences. This work was supported by the National Science Foundation under grant DMR-9807180 and the Beckman Young Investigator program.

References and Notes

- (1) Adachi, T.; Sakka, S. *J. Mater. Sci.* **1990**, *25*, 4732.
- (2) Pekala, R. W.; Hrubesh, L. W.; Tilotson, T. M.; Alviso, C. T.; Pocco, J. F.; LeMay, J. D. In *Mechanical Properties of Porous and Cellular*

- Materials*; Sieradzki, K., Green, D. J., Gibson, L. J., Eds.; MRS Proceedings; MRS: Pittsburgh, PA, 1991; No. 207, p 197.
- (3) Brinker, C. J. *Sol-Gel Science*; Academic Press: Boston, 1990.
 - (4) Kresge, C. T.; Leonowitz, M. E.; Roth, W. J.; Vartuli, J. C.; Beck, J. S.; *Nature* **1992**, *359*, 710. Beck, J. S.; et al. *J. Am. Chem. Soc.* **1992**, *114*, 10834.
 - (5) Jayaraman, A. *Rev. Sci. Instrum.* **1986**, *57*, 1013.
 - (6) Huo, Q.; Margolese, D. I.; Stucky, G. D. *Chem. Mater.* **1996**, *8*, 1147.
 - (7) Gross, A. F.; Ruiz, E. J.; Tolbert, S. H. *J. Phys. Chem. B* **2000**, *104*, 5448.
 - (8) The increase in d spacing at high pressure observed in damp samples is assigned to a transition from Bragg scattering from the hexagonal periodicity to diffuse small angle scattering from the characteristic pore + wall size of the partially collapsed composite. For a hexagonal structure, the pore-to-pore distance is $2/\sqrt{3}$ times larger than the (100) diffraction peak spacing.
 - (9) Tatsumi, T.; Koyano, K. A.; Tanaka, Y.; Nakata, S. *Chem. Lett.* **1997**, 469.
 - (10) Kubo, T.; Ohtani, E.; Kato, T.; Shinmei, T.; Fujino, K. *Science* **1998**, *282*, 85.
 - (11) Gusev, V. Y.; Feng, X. B.; Bu, Z.; Haller, G. L.; O'Brein, J. A. *J. Phys. Chem.* **1996**, *100*, 1985.
 - (12) Koyano, K. A.; Tatsumi, T.; Tanaka, Y.; Nakata, S. *J. Phys. Chem. B* **1997**, *101*, 9436.
 - (13) Jorgensen, J. D. *J. Appl. Phys.* **1978**, *49*, 5473.
 - (14) Grimsditch, M. *Phys. Rev. Lett.* **1984**, *52*, 2379.
 - (15) Lacks, D. J. *Phys. Rev. Lett.* **1998**, *80*, 5385.
 - (16) Gibson, L. J.; Ashby, M. F. *Cellular Solids: Structure and Properties*; Pergamon: Oxford, U.K., 1988. Gibson, L. J. *Mater. Sci. Eng. A* **1989**, *110*, 1.
 - (17) Vukcevic, M. R. *J. Non-Cryst. Solids* **1972**, *11*, 25.
 - (18) An average value of the bulk modulus in the pressure range of 0–3 GPa was calculated using numerical averaging of pressure dependent data [$\kappa(P)$]. For vitreous silica glass, $\kappa_0 = 37$ GPa, but this value decreases as pressure increases. Kondo, K.; Lio, S.; Sawaoka, A. *J. Appl. Phys.* **1981**, *52*, 2826.
 - (19) We used a value of $\kappa_0 = 37$ GPa and $\kappa_0' = 6$ to calculate an average value of the bulk modulus for quartz in the pressure range of 0–3 GPa. Bass, J. D.; Liebermann, R. C.; Weidner, D. J.; Finch, S. J. *Phys. Earth Planet. Inter.* **1981**, *25*, 140.
 - (20) Bloor, D. M.; Gormally, J.; Wyn-Jones, E. *Chem. Soc. Faraday Trans.* **1984**, *80*, 1915.
 - (21) Lacks, D. J. *Phys. Rev. Lett.* **2000**, *84*, 4629.
 - (22) Sigmund, O.; *J. Mech. Phys. Solids* **2000**, *48*, 397.
 - (23) Landmesser, H.; Kosslick, H.; Storek, W.; Fricke, R. *Solid State Ionics* **1997**, *101–103*, 271.
 - (24) Wittlinger, J.; Fischer, R.; Werner, S.; Schneider, J.; Schulz, H. *Acta Crystallogr.* **1997**, *B53*, 745.
 - (25) Hazen, R. M. *Science* **1983**, *219*, 1065.
 - (26) Landman, U.; Luedtke, W. D.; Burnham, N. A.; Colton, R. J. *Science* **1990**, *248*, 454.
 - (27) Wong, E. W.; Sheehan, P. E.; Lieber, C. M. *Science* **1997**, *277*, 1971.
 - (28) Hemley, R. J.; Mao, H. K.; Bell, P. M.; Mysen, B. O. *Phys. Rev. Lett.* **1986**, *57*, 747.
 - (29) Dupree, E.; Pettifer, R. F. *Nature* **1984**, *308*, 523.
 - (30) Lu, Y.; et al. *Nature* **1997**, *389*, 364.
 - (31) Brinker, C. J.; Anderson, M. T.; Ganguli, R.; Lu, Y. Ordered Mesoporous Thin Films. U.S. Patent No. 5,858,457, issued January 12, 1999.
 - (32) Zhao, D.; Yang, P.; Melosh, N.; Feng, J.; Chmelka, B. F.; Stucky, G. D. *Adv. Mater.* **1998**, *10*, 1380.
 - (33) Walker, J. V.; et al. *J. Am. Chem. Soc.* **1997**, *119*, 6921.